Journal of Medical and Biological Engineering (2025) 45:1–12
https://doi.org/10.1007/s40846-025-00928-5

ORIGINAL ARTICLE

A New Approach for Sleep Stage Identification Combining Hidden Markov Models and EEG Signal Processing

Areti Pouliou[1] · Vasileios E. Papageorgiou[1] · Georgios Petmezas[2] · Diogo Pessoa[3] · Rui Pedro Paiva[3] · Nicos Maglaveras[2] · George Tsaklidis[1]

Received: 15 April 2024 / Accepted: 13 January 2025 / Published online: 17 February 2025

Abstract

Purpose Sleep constitutes a third of human life, underscoring its importance in health-related and psychophysiological research. Monitoring sleep stage evolution is critical for understanding sleep-related issues and diagnosing disorders. This study aims to classify sleep stages using a Hidden Markov Model (HMM) based on spectral statistical measures derived from raw electroencephalography (EEG) signals. It explores effective feature combinations to enhance classification accuracy while maintaining a practical approach requiring minimal inputs.

Methods We utilized raw EEG signals to extract various statistical features in the frequency domain, identifying combinations that maximize predictive performance. The proposed HMM was employed to classify sleep stages, leveraging these spectral features. Unlike many prior studies that focus solely on machine learning (ML) techniques, our analysis emphasizes feature significance and model interpretability.

Results Our approach achieved a multiclass classification accuracy of 76.76% using only EEG recordings. This performance demonstrates the utility of spectral statistical features for sleep stage classification, with results comparable to more complex ML methods.

Conclusion The proposed methodology highlights a practical, accurate and interpretable approach to sleep stage classification using EEG data. Its simplicity and efficiency make it suitable for both offline and online applications, supporting improved diagnosis of sleep disorders and advancing sleep research.

Keywords Hidden Markov Models · Spectral analysis · Spectral features · EEG · Signal processing · Sleep stage classification

1 Introduction

Sleep is a fundamental physiological process essential for the overall health and well-being. Sleep disorders are widespread in most of the population and may lead to serious health problems affecting the quality of life [1]. In fact, about 150 million people worldwide are currently suffering from sleep issues [2]. Beyond the immediate impact on sleep quality, such disorders have far-reaching consequences on physical health, cognitive performance and emotional well-being. Chronic sleep deprivation and untreated sleep disorders are associated with an increased risk of developing a wide range of health conditions, including cardiovascular diseases, metabolic disorders, mood disorders and impaired immune function.

Sleep, comprising a third of human existence, underscores its significance in both the study of health-related issues and broader psychophysiological investigations. In 1968, Rechtschaffen and Kales (R&K) [3] introduced the initial sleep stage classification system. This system is one of the foundational and widely recognized frameworks for categorizing sleep stages based on physiological parameters. It primarily distinguishes sleep stages through the analysis of electrophysiological signals obtained from

✉ Vasileios E. Papageorgiou
vpapageor@math.auth.gr

[1] Department of Mathematics, Aristotle University of Thessaloniki, 54124 Thessaloniki, Greece

[2] School of Medicine, Aristotle University of Thessaloniki, 54124 Thessaloniki, Greece

[3] University of Coimbra, CISUC/LASI – Centre for Informatics and Systems of the University of Coimbra, Department of Informatics Engineering, Coimbra, Portugal

polysomnography (PSG). The physiological parameters that are used are: EEG, which records brain wave activity, with specific patterns characterizing different sleep stages (e.g., alpha waves during wakefulness, theta waves in light sleep and delta waves in deep sleep), electrooculogram (EOG), that measures eye movements, identifying rapid eye movements (REM) and slow rolling eye movements in non-REM sleep, and electromyogram (EMG) which assesses muscle tone, which decreases progressively during NREM sleep and becomes nearly absent during REM sleep.

The R&K system defines 5 sleep stages: Stage W (Wakefulness) marked by alpha waves and high muscle tone, Stage N1 (Light Sleep) which is a transition from alpha to theta waves, accompanied by slow eye movements, Stage N2 characterized by theta waves, sleep spindles and K-complexes with minimal eye movement, Stage N3 (Deep Sleep) dominated by high-amplitude delta waves and reduced muscle tone, and Stage REM (Rapid Eye Movement Sleep) which features mixed-frequency EEG activity, rapid eye movements and significant muscle atonia. Sleep stages are scored through visual inspection of 30-s epochs of EEG, electroophthalmogram and electromyogram (EMG) recordings. The R&K system served as the standard for sleep classification until 2007, when the American Academy of Sleep Medicine (AASM) revised the classification, merging Stages 3 and 4 into a unified N3 stage, which is now the accepted standard in sleep medicine.

The proposed approach involved dividing the patient's EEG into 30 s segments and analyzing the EEG rhythms and various parameters for each segment individually. These segments were then categorized into one of the following sleep stages: wake, light sleep (N1), slow-wave sleep (comprising stages N2–N4) and REM. From now on we will denote slow-wave sleep with SWS.

Sleep scoring plays a pivotal role both in sleep research and in clinical practice [4]. Traditionally, this process has relied on manual scoring by human experts. However, such approaches are time-consuming and might result in inconsistencies between different scorers. To overcome some of these difficulties, several automated methodologies have been proposed over the years for the automated sleep scoring. Such methodologies can yield much higher throughput and may also be used for continuous monitoring [4].

The arrangement of sleep stages throughout the night, known as sleep architecture, is influenced by various biological, behavioral and clinical factors. Based on [5], using Bayesian network modeling, it is revealed that sleep architecture is influenced by factors such as time of day, total sleep time, age and gender. Moreover, it is found that the subsequent sleep stage and its duration can be effectively predicted by considering the preceding two stages and age. The duration spent in each sleep stage depends on both age and gender, reflecting variations in biological sleep needs over time and differences between men and women [6]. As individuals age, there is typically a decline in the overall necessity for sleep. Men tend to spend more time in stage 1 sleep and experience increased nighttime awakenings, leading to a heightened risk of daytime sleepiness. Conversely, women tend to maintain longer periods of slow-wave sleep, yet they frequently report difficulties falling asleep, particularly during pregnancy and the early postpartum period, when daytime sleepiness often escalates.

The information derived from EEG signals can offer crucial insights into sleep structure. For instance, time–frequency analysis techniques, commonly employed in sleep analysis, rely solely on EEG data. These techniques enable the identification of changes in EEG dynamics throughout the night, representing a tridimensional function of EEG frequency, EEG power and time. This underscores the potential of EEG signals to provide comprehensive and informative data about sleep architecture, further emphasizing the importance of investigating the viability of EEG-only sleep staging methodologies [7].

Sleep manifests not just in the EEG, but also in the rhythms of the heart and patterns of breathing [8]. A study in [9] involved the measurement of electrocardiograms (ECGs) and breathing patterns in patients with obstructive sleep apnea (OSA), which were then compared with actigraphy data. As a result, it appears that cardiorespiratory signals can offer reasonably accurate means of distinguishing between sleep and wake states, akin to the performance of actigraphy. Moreover, integrating cardiorespiratory-based sleep staging could prove valuable in-home sleep apnea monitoring systems that lack EEG capabilities, enabling them to differentiate between sleep and wake states. Additionally, neural networks have been employed to explore whether transitions between sleep stages yield insights into sleep consistency and its impact on sleep quality [10]. The classification of sleep stages is conducted by first examining the processing of EEGs, EOGs, EMGs and ECGs.

What sets the present research apart from the majority of studies in the literature, is that it focuses on building an HMM solely based on EEG-derived signals. The necessity of only EEG recordings, which can be easily retrieved from patients, enhances the applicability of our approach. By relying solely on EEG data, the proposed model necessitates the existence of less information to draw direct inferences about the distribution of sleep stages. Another new element of the present analysis is that the criteria for defining the hidden states are established through the computation and analysis of statistics derived from spectral features generated from the power spectrum of the EEG signals. Finally, our methodology involves a novel process: calculating statistical characteristics of the EEG signal's power spectrum using Fast Fourier Transform (FFT), and subsequently establishing thresholds to classify different sleep stages. This approach,

which is up to now unexplored in existing literature, suggests the promising potential of HMMs in the classification of sleep stages.

2 Related Work

In general, HMMs have been used in several fields concerning medical applications [11, 12], seismicity data [13], biological and environmental modelling [14, 15]. The examined phenomenon is usually described using discrete states, while through HMM methodology we aim to extract valuable information after processing the transition pattern between them. Apart from that kind of applications, HMMs have a presence in psychology too. They have found particular utility in the realms of learning and memory [16]. Within the domain of learning, Markov models exhibit notable adaptability, effectively capturing and structuring the progression of knowledge. HMMs have diverse applications across several fields due to their capability to model sequential data with hidden states. The authors in [17] describe how HMMs can be employed in biological sequence analysis and how they can be used to analyze RNA sequences. Various articles apply HMM to speech recognition, like the one presented in [18], where it is explained that speech recognition systems that rely on HMMs are contingent upon several assumptions. One such assumption is that speech signals can be sufficiently represented by a series of feature vectors derived from spectral analysis.

Brain functional connectivity, closely related to brain activity, provides insights into the interaction between brain areas. In [19], EEG-based brain mechanisms of sleep stages are explored through functional connectivity, particularly focusing on different frequency bands using the phase-locked value (PLV) method. Brain interactions during sleep stages are being analyzed, and the performance of different frequency bands for sleep stage classification is being evaluated using feature-level, decision-level and hybrid fusion methods.

Various neural networks play a role in controlling sleep cycles and alertness. Also, deep neural networks are being used for processing large data extracted from polysomnography in [20]. In [21], various classifiers are developed and tested on three distinct datasets, each comprising healthy individuals with different sleep patterns. The authors in [22] examine the variability in sleep patterns through the analysis of heart rate variability within the autonomic nervous system. The research reveals that the combined duration of different sleep stages, including light, deep and REM sleep, follows an exponential distribution characterized by a specific time scale, while the duration of brief awakenings during sleep adheres to a scale-free power-law distribution. In [23], the authors utilized deep learning techniques to develop an algorithm for automated sleep stage classification, leveraging the time series data of instantaneous heart rate (IHR) obtained from ECG signals.

The classification of sleep into distinct stages is a valuable technique in the investigation of sleep disorders. In [24], FIR filters are employed to extract EEG rhythms, and sleep classification is carried out using Random Forests, achieving an accuracy of 75.29%. Likewise, in another study [25], polysomnogram data are analyzed using Fourier transform (FT). These data are then subjected to statistical processing, along with paired t-tests, to determine the likelihood of epileptic seizures occurring during specific sleep stages.

The issue of inaccessible algorithms in proprietary software is addressed in [26], where a solution involves the development of open-source software. This software is accompanied by an algorithm that has been trained using a dataset comprising 30,000 h of polysomnograms. The performance of this algorithm is then compared with two other algorithms using a dataset consisting of patients diagnosed with OSA.

A comparable investigation is conducted in [10], wherein polysomnograms from 20 patients are examined. These signals were segmented based on the R&K rules and transformed into frequency data using Laplace transforms. Subsequently, they were categorized into five states: Wake, S1, S2, SWS and REM. An approach for tracking human sleep–wake patterns using HMMs is outlined in [21]. In this study, actigraphy, a non-invasive technique for monitoring human rest and activity cycles employing accelerometers, is employed to collect data from 43 samples. The accelerometer-derived data is logarithmically converted and categorized into "Sleep" and "Wake" phases. Finally, another study employing HMMs, focusing on sleep disorders, particularly the identification of apnea, is discussed in [20]. This research utilizes nocturnal oximetry, a method for monitoring arterial oxygen saturation $\left(SaO_2\right)$ during sleep, which is regarded as a robust tool for detecting sleep apnea. The study involves the analysis of oximetric data from 128 subjects, classifying it into three categories of apnea, namely OSA, hypopnea and central apnea.

3 Methodology

In this section, we present the mathematical models, techniques and preprocessing steps employed for the sleep stage classification procedure. To begin, we delve into the mathematical underpinnings of HMMs. Next, we discuss the processing pipeline of the EEG signal and lastly, we provide an overview of key aspects in the domain of frequency and spectral analysis.

3.1 Hidden Markov Models

An HMM represents a dual stochastic Markov process, one of which is hidden and cannot be directly observed, but instead, it generates a sequence of observable events. An HMM comprises a collection of hidden states, a set of observed states and three sets of probabilities: the transition probabilities ($\boldsymbol{P}$), the probabilities of emission or occurrence of observable states ($\boldsymbol{B}$), and the initial probabilities ($\boldsymbol{\pi}$). It is conventionally denoted as λ, which encompasses these three sets of probabilities. The HMMs can be utilized for the examination of the following tasks, i.e.,

1. *Valuation problem*: Determining the most efficient method for computing the probability $P[O|\lambda]$, which represents the likelihood of generating a specific observed sequence $\mathrm{O} = \{o_1, o_2, \ldots, o_\mathrm{T}\}$ based on the probability model λ. This probability quantifies how closely the model aligns with the observations and proves valuable when faced with multiple potential models, aiding in the selection of the most suitable one.
2. *Decryption problem*: Identifying the best (with the highest likelihood) sequence of hidden states, based on the observed sequence O and model λ.
3. *Estimation problem*: Adjusting the model parameters λ in a manner that maximizes $P[O|\lambda]$. This process aims to attain the most accurate representation of the phenomenon under study, a goal pursued with each respective model.

In this research, the second problem of HMMs is solved with the help of the Viterbi algorithm. According to the Viterbi methodology we determine the sequence of hidden states with the maximum likelihood given a sequence of observable states. Let

$$\begin{aligned}\delta_t(i) &= max_{X_1,\ldots,X_{t-1}} P\left[X_1, \ldots, X_{t-1}, X_t = i, y_1, \ldots, y_t|\lambda\right] \\ &= \left[max_{1\le j\le N}\delta_{t-1}(j)p_{ij}\right]b_i\left(y_t\right).\end{aligned} \tag{1}$$

We initiate the algorithm as

$$\delta_1(i) = \pi_i b_i\left(y_1\right), \quad 1 \le i \le N, \tag{2}$$

$$\psi_i(1) = 0. \tag{3}$$

Inductively,

$$\delta_t(i) = [max_{1\le j\le N}\delta_{t-1}(j)p_{ij}]b_i\left(y_t\right), \quad 2 \le t \le T, 1 \le i \le N, \tag{4}$$

$$\psi_t(i) = arg_{1\le j\le N} \max\left[\delta_{t-1}(j)p_{ji}\right], \quad 2 \le t \le T, 1 \le i \le N. \tag{5}$$

where $b_i\left(y_t\right)$ are the emission probabilities of observing y_t considering that we have the hidden state i. The Viterbi algorithm terminates when

$$\hat{P} = max_{1\le j\le N}\delta_T(j), \tag{6}$$

and

$$\hat{X}_T = arg_{1\le j\le N} \max\left[\delta_\mathrm{T}(j)\right], 1 \le t \le T. \tag{7}$$

Therefore, we lead to the estimation of the sequence of the hidden states based on

$$\hat{X}_t = \psi_{t+1}\left(\hat{X}_{t+1}\right), \quad t = T-1, \ldots, 1. \tag{8}$$

Incorporating hidden states in the model renders it sufficiently adaptable to tackle a range of complex real-world issues, while maintaining the Markov property enables the employment of efficient computational techniques.

3.2 Statistical Signal Analysis

3.2.1 Fourier Transform

Fourier analysis transforms a signal from its original domain (often time) to a representation in the frequency domain and vice versa. The discrete Fourier transform (DFT) is obtained by decomposing a sequence of values into components of different frequencies. Let $x_0, x_1, \ldots, x_{N-1}$ be complex numbers. Then, the DFT is defined as

$$X_k = \sum_{n=0}^{N-1} x_n e^{-i2\pi kn/N}, \tag{9}$$

where N is the cardinality of data points, while $k = 0, \ldots, N-1$.

In signal processing, DFT is extensively used in tasks such as filtering, spectral analysis and feature extraction. It allows analyzing the frequency components of a signal, which is crucial in various applications like audio processing, image processing and communications. In spectral analysis, DFT is employed for analyzing the frequency content of a signal, which is essential in applications like vibration analysis, EEG signal analysis in neuroscience and power spectrum estimation in electrical engineering. In image processing, DFT is used for tasks such as image compression, image enhancement and pattern recognition. It helps in transforming images from the spatial domain to the frequency domain, where operations like filtering and analysis become more efficient. Also, DFT plays a crucial role in audio processing applications such as speech recognition, audio compression and equalization. Lastly, in medical imaging techniques such as magnetic resonance imaging (MRI) and computed tomography (CT) scans for image

reconstruction and analysis, DFT aids in processing the raw data acquired from medical imaging devices to generate meaningful images [27].

3.2.2 Power Spectrum

A power spectrum characterizes the frequency content and resonances within a system, that is, it describes how the intensity of a time-varying signal is distributed in the frequency domain. The graph of the power spectrum for a continuous signal, is made based on the mathematical formula

$$S(f) = \left| \int_0^{\infty} x(t) e^{-2\pi i f t} dt \right|^2 \approx \int_{-\infty}^{\infty} R(\tau) e^{-2\pi i f \tau} d\tau, \tag{10}$$

where $R(\tau) = \lim_{T\to\infty} \frac{1}{T} \int_{-\infty}^{\infty} x(t)x^*(t-\tau)dt$, represents the autocorrelation function and $x^*(t)$ the complex conjugate of $x(t)$. Therefore, the power spectrum is defined as the plot of the square of the absolute value of the amplitude of FT with respect to the signal's frequencies.

3.2.3 Statistical Measures of Power Spectrum

For the power spectrum function, a series of statistical characteristics are calculated, namely the Spectral Centroid, Spectral Spread, Spectral Skewness, Spectral Kurtosis, Spectral Entropy, Spectral Flatness, Spectral Crest and Spectral Slope. The mathematical formulas associated with the computation of the aforementioned measures are presented in Table 1.

We note that s_k and f_k represent the spectral value and the respective frequency of the spectrum at the k-th bin, b_1 and b_2 are the bounds within which (e.g.) the slope is computed for a given data set. Moreover, μ_1 denotes the spectral centroid, μ_2 the spectral spread, μ_f the mean frequency and μ_s the mean spectal value. In numerous analyses, characteristic EEG features extracted from the frequency spectrum –such as Delta, Theta, Alpha, Beta and Gamma rhythms—have been utilized as crucial components for effective pattern recognition and disease classification [28–30]. However, in our scenario, these features do not furnish adequate information for sleep stage classification. This is due to the fact that during sleep, we typically observe only Delta and Theta waves. This fact led to experimentation with the aforementioned alternative statistical measures.

To analyze the statistical properties of the mentioned spectrum characteristics and present the produced results, the R processing language is employed. This involves utilizing the Tukey test for statistical analysis and generating boxplots for data visualization. The Tukey test (or HSD-Honestly Significant Difference) statistic is a one-step,

Table 1 Statistical measures of power spectrum

Spectral statistical measure	Mathematical formulas
Spectral centroid	$\mu_1 = \frac{\sum_{k=b_1}^{b_2} f_k s_k}{\sum_{k=b_1}^{b_2} s_k}$
Spectral spread	$\mu_2 = \sqrt{\frac{\sum_{k=b_1}^{b_2} (f_k-\mu_1)^2 s_k}{\sum_{k=b_1}^{b_2} s_k}}$
Spectral skewness	$\mu_3 = \frac{\sum_{k=b_1}^{b_2} (f_k-\mu_1)^3 s_k}{(\mu_2)^3 \sum_{k=b_1}^{b_2} s_k}$
Spectral kurtosis	$\mu_4 = \frac{\sum_{k=b_1}^{b_2} (f_k-\mu_1)^4 s_k}{(\mu_2)^4 \sum_{k=b_1}^{b_2} s_k}$
Spectral entropy	$entropy = \frac{-\sum_{k=b_1}^{b_2} s_k log(s_k)}{log(b_2-b_1)}$
Spectral flatness	$flatness = \frac{\left(\prod_{k=b_1}^{b_2} s_k\right)^{\frac{1}{b_2-b_1}}}{\frac{1}{b_2-b_1}\sum_{k=b_1}^{b_2} s_k}$
Spectral crest	$crest = \frac{max\left(s_{k\in[b_1,b_2]}\right)}{\frac{1}{b_2-b_1}\sum_{k=b_1}^{b_2} s_k}$
Spectral slope	$slope = \frac{\sum_{k=b_1}^{b_2} (f_k-\mu_f)(s_k-\mu_s)}{\sum_{k=b_1}^{b_2} (f_k-\mu_f)^2}$

multiple-comparison procedure based on the Student's t-distribution that can be used to find means that are significantly different from each other. The formula for the statistic of the Tukey-test is

$$q_s = \frac{Y_A - Y_B}{SE}, \tag{11}$$

where Y_A and Y_B represent the larger and smaller of the two mean values being compared, while SE is the standard error of the sum of the means.

The confidence limits for all pairwise comparisons using the Tukey test with a confidence coefficient of at least $1-\alpha$, where α corresponds to the significance level, can be computed based on

$$\bar{y}_{i.} - \bar{y}_{j.} \pm \frac{q_{a;k;N-k}}{\sqrt{2}} \hat{\sigma}_\varepsilon \sqrt{\frac{1}{n_i} + \frac{1}{n_j}}, \tag{12}$$

where n_i and n_j represent the sample sizes of the compared groups, $\bar{y}_{i.}$ and $\bar{y}_{j.}$ are the respective mean values, while $\hat{\sigma}_\varepsilon$ is the standard deviation of the entire design. In case where we have groups of the same size, formula (12) is modified as

$$\bar{y}_{i.} - \bar{y}_{j.} \pm q_{a;k;N-k} \frac{\hat{\sigma}_\varepsilon}{\sqrt{n}}. \tag{13}$$

Figure 1 shows a diagrammatic representation of the introduced preprocessing procedure followed by the classification methodology based on hidden Markov modelling.

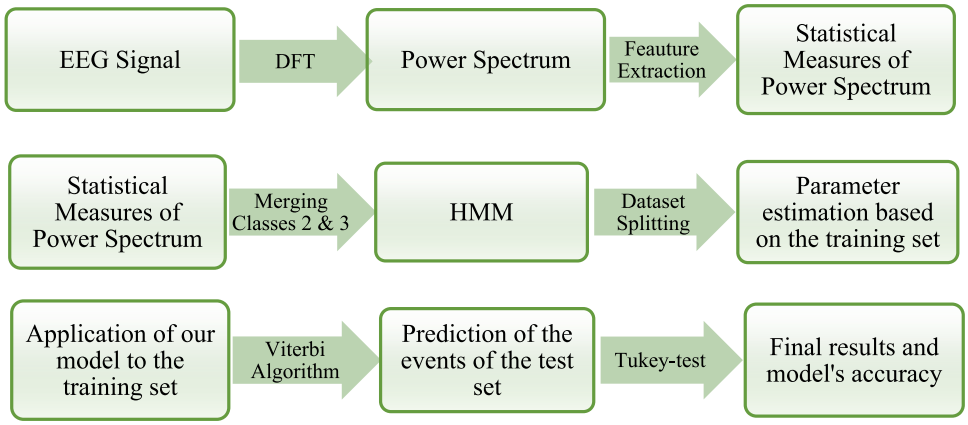

Fig. 1 Flowchart presenting the developed preprocessing steps and classification procedure

3.2.4 Dataset

The sleep-edf database [31] utilized in this study comprises 197 full-night Polysomnographic sleep recordings, incorporating EEG, EOG, chin EMG and event markers. Some of these recordings also feature respiration and body temperature data. Hypnograms, representing sleep patterns, were meticulously scored by proficient technicians following the R&K manual and are accessible as well.

The Polysomnographic sleep recordings encompass EEG data (from Fpz-Cz and Pz-Oz electrode placements), EOG (horizontal), submental chin EMG and annotated sleep stages (events). Additional data such as oro-nasal respiration and rectal body temperature are present in some recordings. Certain files include annotations indicating sleep stage patterns corresponding to the PSGs. These patterns, also known ashypnograms, encompass the following sleep stages: wake (W), REM (R), N1, N2, N3 and N4. We note that N3 and N4 are considered as one phase (SWS) in most analysis, as they do not exhibit significant differences. Also, as we mentioned in the introduction, for the purposes of our analysis we include N2 to the SWS phase, as these three sleep stages correspond to deep sleep. All hypnograms were manually scored by trained technicians following the guidelines outlined in the 1968 R&K manual, based on Fpz-Cz/Pz-Oz EEG recordings.

In this research we used only the EEG from Fpz-Cz and Pz-Oz electrode locations from the sleep recordings of two individuals. The dataset consists of healthy individuals who are not on any medication, which is a key factor for this study. In other circumstances, the presence of medical or mental conditions could produce different results. Nonetheless, the inclusion of patients with mental illnesses that affect their sleep cycles, along with extensive comparisons to healthy individuals, could be interesting for future work, offering valuable insights into the phenomenon being examined. The full-night recording starts 30 min before the subjects fall asleep and stops 30 min after they wake up. Each EEG signal is segmented into 30 s intervals, with a sampling rate of 100 Hz. As a result, for every 3000 EEG signal time steps there is an event which describes the individual's sleep stage. Ultimately, a timeseries of 2040 events that represent the observable states of the HMM is derived.

4 Results

Initially, the above-mentioned segmentation approach is applied. Subsequently, power spectrum diagrams were generated using Fourier transformations within the MATLAB programming environment, presented in Fig. 2. For each of the 2040 events we computed the previously mentioned statistical properties. This included calculating the mean, minimum and maximum values for these properties. Additionally, we subjected these values to the Tukey test and visualized the results through graphical representations.

In the initial phase of our research, the statistical test indicated that there are no statistically significant differences between sleep stages N2 and SWS. Consequently, for the continuation of the study, we include stage N2 in the class (phase) SWS which represents state 3. As a result, the hidden states in our model are now four, namely state 1 (Wake), state 2 (N1), state 3 (SWS) and state 4 (REM). According to this, the examined dataset contains 441 (21.62%), 612 (30%), 542 (26.57%) and 445 (21.81%) events corresponding to these 4 states, respectively, providing a quite balanced dataset.

Now, we proceed to the determination of the system's observable states. Through our graphical analysis, we discovered that the values of five statistical characteristics, namely Mean Skewness, Mean Slope, Min Skewness, Max Flatness and Min Slope, play a significant role in forming the set of observable states. As we earlier mentioned, during the experimentation phase, we computed a series of eight fundamental spectral features (Table 1). The Mean Slope and Min Slope values across all 2040 EEG segments

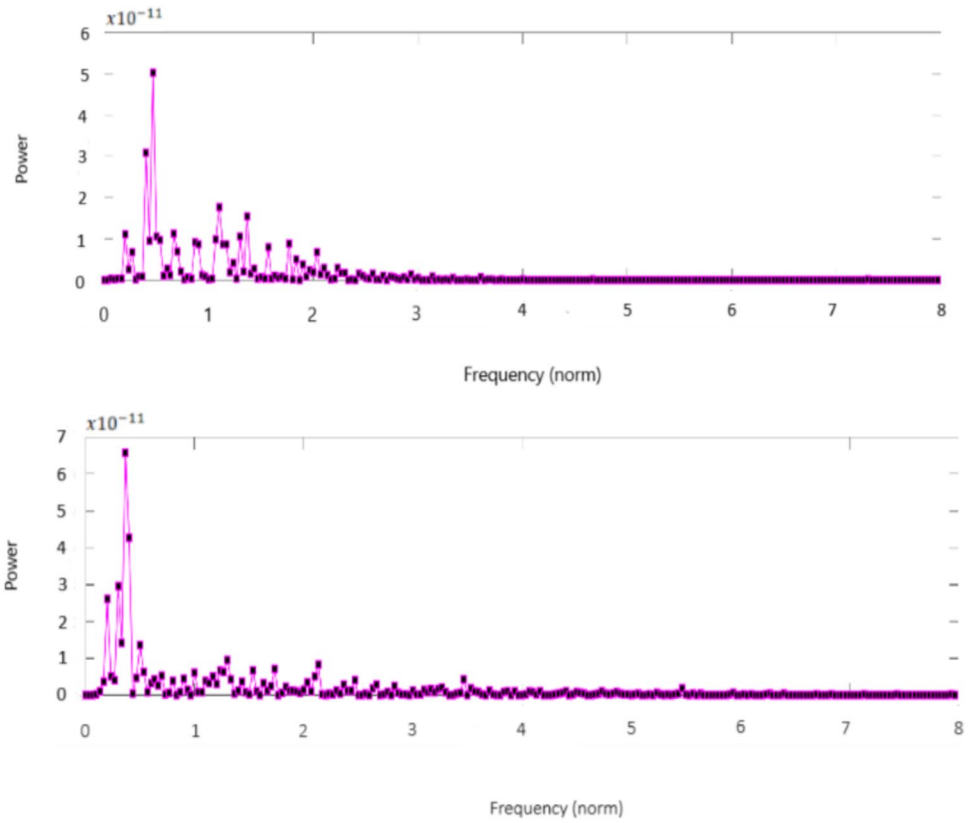

Fig. 2 Power spectrum diagrams that correspond to the EEG signals of the examined individuals

were close to zero. This derives from the properties of this spectral feature. EEG signals exhibit a "1/f" power distribution, meaning the power decreases with increasing frequency. The slope isn't steep in most EEG signals because the power does not drop drastically across the frequency spectrum. EEG signals are dominated by specific frequency bands, such as delta, theta, etc. The overlap and relative stability of these bands often produce a spectral slope near 0. Therefore, to simplify handling and avoid dealing with numbers containing numerous decimal places, we normalized these values. We employed the standard transform

$$x_{norm} = \frac{x - x_{min}}{x_{\max} - x_{min}}, \tag{14}$$

where in our case x represents the Mean Slope values.

Next, we analyzed the values of each feature to identify those that provide notable distinctions between the system's hidden states. The goal of this process was to improve the classification performance of the HMM. A combination of the Tukey test and boxplot graphical analysis was applied to identify the five statistical characteristics that significantly influence the determination of the observable states in our model. After a thorough examination of the boxplot graphics for each characteristic, we concluded that the selected values—Min Skewness, Mean Skewness, Max Flatness, Norm. Mean Slope and Norm. Min Slope—are the most effective in accurately determining the patients' sleep stages. After extensive experimentation, the construction of the final model's observable states was generated by considering combinations of attribute values with respect to the Min Skewness and Max Flatness. Specifically, the final model's four observable states were determined based on:

- ***obs1***: Min Skewness > 100 & Max Flatness ≤ 0.8
- ***obs2***: Min Skewness > 100 & Max Flatness > 0.8
- ***obs3***: Min Skewness ≤ 100 & Max Flatness ≤ 0.8
- ***obs4***: Min Skewness ≤ 100 & Max Flatness > 0.8.

We divided the 2040 events into two subsets: the first (training) and second (test) subsets contained 1700 and 340 events, respectively. Based on the training subset we estimated the model's parameters, while for the second subset (340 events) we applied the Viterbi algorithm to predict the corresponding hidden states. The Viterbi algorithm achieved correct predictions for 261 out of the 340 observations, providing an accuracy rate of 76.76%.

In a subsequent experimentation phase, the generation of observable states is investigated using all pairs resulting from the combinations of the 5 statistical characteristics,

pairing them two at a time. The following thresholds are selected based on the visual examination of boxplot diagrams, i.e.:

- Mean Skewness ≤ 6, $6 <$ Mean Skewness ≤ 7.5, Mean Skewness > 7.5
- Min Skewness ≤ 100, Min Skewness > 100
- Norm. Mean Slope ≤ 0.858, Norm. Mean Slope > 0.858
- Norm. Min Slope ≤ 0.7, Norm. Min Slope > 0.7
- Max Flatness ≤ 0.8, Max Flatness > 0.8.

After the visual inspection, the Tukey test has been employed aiming to validate that the chosen thresholds provide statistically significant differentiation which aids the identification of different hidden states.

It appears that the models using the observable states derived from the pairs Min Skewness—Norm. Min Slope and Min Skewness—Max Flatness provided the highest performance, achieving an accuracy of approximately 76.76%. Another notable result was obtained from models using the pairs Mean Skewness—Norm. Min Slope and Mean Skewness—Max Flatness, which achieved a slightly lower but still satisfactory accuracy of 75.59%. In a final, third phase, observable states were generated based on combinations of the 5 characteristics taken three at a time, resulting in the outcomes displayed in Table 2.

When using three statistical features, we have found that cardinality of observable states ranges between 2 and 9. We note that the observable states of the HMM are connected to the hidden states based on the emission probabilities ($b_i(y_t)$). As outlined in the methodology, HMMs are composed of a series of hidden states, a set of observed states and three probability distributions. The number of observable states is presented in Tables 2 and 3, as they have occurred depending on the pair or triplet of statistical characteristics employed for each model instance.

Table 3 Combination of the statistical characteristics in pairs and their performance

Pairs of spectral features	Number of observable states	Accuracy (%)
Mean Skewness-Min Skewness	6	47.94
Mean Skewness-Norm. Min Slope	6	75.59
Mean Skewness-Norm. Mean Slope	3	47.94
Mean Skewness-Max Flatness	6	75.59
Min Skewness-Norm. Mean Slope	3	50.88
Min Skewness-Norm. Min Slope	3	76.76
Min Skewness-Max Flatness	3	76.76
Norm. Mean Slope-Max Flatness	4	22.35
Norm. Min Slope-Max Flatness	2	47.94

For instance, considering the triplet Mean Skewness, Min Skewness and Norm. Min Slope, the maximum possible number of observable states (combinations) is 12. However, for 3 parameter combinations, namely (Mean Skewness ≥ 7.5, Min Skewness > 100, Norm. Min Slope < 0), (Mean Skewness ≤ 6, Min Skewness > 100, Norm. Min Slope ≤ 0) and ($6 \leq$ Mean Skewness < 7.5, Min Skewness > 100, Norm. Min Slope ≤ 0), there are no hidden states which correspond to these aforementioned observable states. As a result, the cardinality of observable states decreases from 12 to 9.

Comparing the results from Tables 2 and 3, it is evident that the HMM algorithm's accuracy rates do not significantly differ, with the highest percentage still being 76.76%. We highlight once again, that the highest accuracy was achieved when combining values of the statistical

Table 2 Triple combinations of the spectral statistical features and their performance

Triplets of spectral features	Number of observable states	Accuracy (%)
Mean Skewness-Min Skewness-Norm. Min Slope	9	75.59
Mean Skewness-Min Skewness-Norm. Mean Slope	6	47.94
Mean Skewness-Min Skewness-Max Flatness	9	75.59
Mean Skewness-Norm. Min Slope-Mean Slope	6	50.88
Mean Skewness-Norm. Min Slope-Max Flatness	6	76.76
Mean Skewness-Norm. Mean Slope-Max Flatness	6	76.76
Min Skewness-Norm. Min Slope-Max Flatness	3	76.76
Min Slope-Norm. Mean Slope-Max Flatness	2	47.94
Min Skewness-Norm. Mean Slope-Max Flatness	3	76.76

characteristics related to spectral Skewness, Slope and Flatness.

5 Discussion and Conclusions

The EEG signals recorded during sleep phases play a pivotal role in both clinical and research domains. Its significance extends to the realms of diagnosing sleep-related disorders, advancing our comprehension of the intricacies of sleep physiology, and facilitating the formulation of efficacious therapies and interventions aimed at enhancing and sustaining wholesome sleep patterns, consequently contributing to the overall health and well-being of individuals [32, 33].

The examination of sleep can rely on different approaches, involving the analysis of distinct signals like those from the brain, heart, breath and muscles, either individually or in combination. On the contrary, the present study focuses exclusively on the analysis of sleep EEGs using HMMs. This approach sets our research apart from others that typically utilize a blend of EEG, EOM and EMG signals to derive their findings, making it a distinctive aspect of this manuscript. An additional innovative aspect of the proposed HMM lies in the approach taken to generate its parameters. Instead of conventional methods [34], we calculated the statistical attributes of the EEG power spectrum derived from our dataset. We then used these statistics to establish threshold values which are later utilized to determine the model's classes. This involved statistical analysis using the Tukey test and visualizing the outcomes through boxplot diagrams, which ultimately shaped the final observable states. Interestingly, the specific combination of statistical characteristics appeared to influence the model's performance during the training and test process, positively impacting its overall precision.

Throughout the test phase, the proposed model demonstrated a satisfactory accuracy of 76.76% using a combination of the statistics from only two spectral features: Min Skewness and Norm. Min Slope, or Min Skewness and Max Flatness. The achieved accuracy is calculated as the ratio of correctly identified events (sleep phases) to the total number of events in the test set. Although multiple models reach this level of accuracy, we recommend these two, as they rely on only two statistical characteristics, thus reducing computational complexity and minimizing the risk of overfitting. Specifically, these are the models based on Min Skewness-Norm. Min Slope and Min Skewness-Max Flatness. This suggests that it is suitable for application in a sleep classification study.

The roles of the maximum, minimum and mean statistics for the selected spectral features are as follows: To compute a spectral feature from an EEG segment, the standard procedure involves applying the FFT to several overlapping windows within the segment. This process generates multiple feature values for each segment. To consolidate these multiple values into a single representative value, we use three key statistics: the mean, maximum and minimum. This step is essential for defining feature cutoff points and identifying observable states, which are necessary for the operation of HMMs. Based on this approach, emphasis should be placed on the physiological significance of the eight selected spectral features, particularly spectral slope, skewness and flatness, as these provided the most accurate classification results.

The eight selected spectral features have significant physiological meaning in the field of sleep stages [35]. First of all, the spectral centroid represents the "center of mass" of the power spectrum and reflects the average frequency of a signal. In the context of sleep stages, lower values indicate deeper non-REM sleep, corresponding to SWS phase, characterized by slow-wave delta activity (0.5–4 Hz). Conversely, in lighter sleep stages such as N1 and wakefulness, the centroid is higher due to increased alpha (8–12 Hz) and beta (13–30 Hz) activity [36]. Spectral spread captures the variance or "width" of the spectrum around its centroid, indicating the range of frequencies in the signal. In phase SWS, the values of spectral spread are reduced because low-frequency delta waves dominate, producing a concentrated spectral profile. Wakefulness has the widest spread due to contributions from alpha, beta and gamma bands, reflecting the broad and varied cortical activity associated with alertness and cognitive processing.

Spectral kurtosis quantifies the "peakedness" of the power spectrum, identifying how much of the power is concentrated in sharp peaks [37]. Higher kurtosis is observed in the SWS stage due to concentrated delta band, creating a strong, single-peak distribution. REM sleep has a lower kurtosis as power spreads across both theta and low beta frequencies, leading to a less peaked spectral profile. Spectral entropy measures the randomness of the frequency distribution. In REM sleep, spectral entropy increases as the frequency distribution becomes more varied reflecting greater cortical processing. Wakefulness typically has the highest entropy due to a complex, distributed power spectrum across a range of frequencies. Spectral crest assesses the degree to which a few frequencies dominate the spectrum. In non-REM sleep (SWS), spectral crest is high as delta waves dominate the EEG signal, forming a sharp peak in the low frequencies. REM sleep shows a moderate spectral crest due to contributions from theta waves, which are prominent but less dominant than delta waves in deep sleep. Wakefulness tends to have a lower spectral crest, as power is more evenly distributed across multiple frequency bands.

Finally, we describe the physiological meaning of the three spectral features that correspond to the models that

provided the maximum accuracy considering pairs of spectral statistics. These features are the spectral skewness, slope and flatness. To begin with, in SWS skewness is usually positive, as delta waves dominate the EEG signal, concentrating power at lower frequencies [38]. REM sleep, with its higher theta (4–8 Hz) activity, tends to have a more balanced distribution, resulting in lower skewness. During wakefulness, skewness is typically lower still, as high-frequency alpha and beta bands have a greater presence, creating symmetric frequency distributions.

Spectral slope indicates how rapidly power decreases as frequency increases, generally computed from a log–log power spectrum. In REM sleep, the slope is less steep because of increased mid-range theta power. In deep non-REM sleep, the spectral slope is steeper due to a dominance of low-frequency delta activity and minimal high-frequency content, reflecting slower cortical activity. In wakefulness, the slope flattens further due to significant power in higher frequency bands like alpha, beta, and even gamma, which are associated with alertness and active brain processing. Finally, spectral flatness measures how evenly power is distributed across frequencies, distinguishing between concentrated (low flatness) and broad (high flatness) spectral content. During SWS flatness is low because power is highly concentrated in the delta range, reflecting synchronous, slow brain activity. In REM phase, flatness increases slightly as theta and low-beta bands contribute, distributing power across a broader frequency range. Wakefulness has the highest flatness as power spreads across alpha, beta and gamma bands, indicating a more complex and variable EEG signal.

All eight features clearly offer valuable insights for distinguishing sleep stages. However, we prioritize the statistics (or feature thresholds) of spectral flatness, skewness and slope, as they yielded the most effective state differentiation for our dataset. Notably, this is the first study to utilize these spectral features for sleep stage classification via a computationally efficient stochastic method like HMM. While the cutoff points might vary with a different dataset, the preprocessing and classification approach is both robust and easily reproducible, facilitating the selection of new feature thresholds. This statement summarized the main contribution of the introduced analysis.

It becomes evident that by employing the Viterbi algorithm, our model can effectively predict the specific sleep stages of a patient, while the respective level of accuracy should be deemed significant, considering the fact that it deals with a multiclass classification task. After dividing the 2040 events into two subsets—one for training and one for test – the model's parameters were estimated using the training subset. For the test subset, consisting of 340 events, the Viterbi algorithm was employed to predict the corresponding hidden states. In both models, which utilized observable states derived from the pairs Min Skewness—Min Slope and Min Skewness—Max Flatness, the Viterbi algorithm accurately predicted 261 out of the 340 observations, resulting in an accuracy rate of approximately 76.76%. Consequently, it holds great promise for research pertaining to the analysis of human sleep, especially when dealing exclusively with sleep EEG data.

We notice this level of accuracy for other four models where the observable states are constructed using triplets of spectral features (Table 2). The creation of multiple models with identical testing accuracy may stem from the observable states being derived from pairs and triplets of the same spectral statistics, which offer the highest distinguishing efficiency for the hidden states. As part of future research, we plan to incorporate additional time and frequency features derived from other signals, such as EOG or EMG. By applying the established preprocessing steps to these signals, we aim to enhance classification performance further [39].

Certainly, it is important to acknowledge that the developed model does have certain limitations primarily tied to data availability. The sample size of the examined time series seems satisfactory, considering that we employ a low-complexity statistical methodology like the HMMs. However, applying the current methodology to EEG recordings from a larger cohort of individuals presents an intriguing direction for further investigation, which we intend to pursue in future work. Furthermore, our analysis could employ a greater collection of the statistical measures derived from the power spectrum or even add time-related measures. It is conceivable that additional features processed in a similar manner, could yield valuable insights.

Additionally, the ranges we established for categorizing each spectral feature may vary based on the numerical scales depicted in the boxplots. It would be intriguing to explore the use of the Viterbi algorithm in our model with a distinct partitioning of the 2040 events. This investigation could shed light on the significance of this segmentation, and identify under which circumstances the algorithm performs optimally, leading to higher accuracy rates. Ultimately, we note that the main purpose of the present analysis is the introduction of a new combination of statistical measures with a Markov-based algorithm, which can provide significant predictive performance regarding sleep-related tasks. The presented analysis can be easily extended in larger datasets or modified classification issues.

Finally, the proposed model has the potential to serve as an initial foundation for research on sleep analysis that can be expanded to various domains, not limited to stage classification. For instance, it could be extended to investigations of sleep disorders, given that our dataset comprises data from healthy individuals, making the outcomes a valuable benchmark for distinguishing between normal and abnormal sleep patterns. In essence, the innovative development of this model offers a valuable resource to enhance the quality

of both new and existing sleep studies, with the overarching goal of continually refining and advancing their outcomes. As future research, it would be intriguing to examine the performance of additional AI or ML algorithms emphasizing low-complexity architectures, which show robustness against phenomena of overfitting [40–45].

Author Contributions Methodology: A.P, V.E.P.; Conceptualization: V.E.P., Data Curation: V.E.P.; Software: A.P., V.E.P.; Writing Original Draft: A.P.; Revise Original Draft: V.E.P., G.P., D.P; Supervision: G.T., R.P.P., N.M.

Funding This research was funded by the Special Account for Research Funds of Aristotle University of Thessaloniki (AUTH) and through national funds by FCT - Fundação para a Ciência e a Tecnologia, I.P., in the framework of the Project UIDB/00326/2025 and UIDP/00326/2025.

Data Availability The utilized dataset exists in the "Sleep-EDF Dataset" of PhysioNet and can be accessed through the link https://www.physionet.org/content/sleep-edfx/1.0.0/.

Declarations

Conflict of interest The authors declare no competing financial interests.

Consent for Publication The data are included in a public repository.

Consent to Participate All recordings included in the PhysioNet dataset were contributed with the subjects' consent.

Informed Consent All the authors have approved the manuscript and the submission.

References

1. Panossian, L. A., & Avidan, A. Y. (2009). Review of sleep disorders. *Medical Clinics of North America, 93*(2), 407–425. https://doi.org/10.1016/j.mcna.2008.09.001
2. Borbély, A. A., Daan, S., Wirz-Justice, A., & Deboer, T. (2016). The two-process model of sleep regulation: A reappraisal. *Journal of Sleep Research, 25*(2), 131–143. https://doi.org/10.1111/jsr.12371
3. Rechtschaffen, A., & Kales, A. (1968). *A Manual of Standardized Terminology*. Public Health Service, US Government Printing Office, Washington DC.
4. Abdelrahman, R., Anna, B. S., & Lisa, G. (2024). The pros and cons of using automated sleep scoring in sleep research: Comparative analysis of automated sleep scoring in human and rodents: advantages and limitations. *Sleep, 47*(1), zsad275. https://doi.org/10.1093/sleep/zsad275
5. Yetton, B. D., McDevitt, E. A., Cellini, N., Shelton, C., & Mednick, S. C. (2018). Quantifying sleep architecture dynamics and individual differences using big data and Bayesian networks. *PLoS One, 13*(4). https://doi.org/10.1371/journal.pone.0194604.
6. Patel, A. K., Reddy, V., Shumway, K. R., et al (2024). Physiology, Sleep Stages. *StatPearls Treasure Island*. https://www.ncbi.nlm.nih.gov/books/NBK526132/.
7. Lambert, I., & Peter-Derex, L. (2023). Spotlight on sleep stage classification based on EEG. *Nature and Science of Sleep, 15*, 479–490. https://doi.org/10.2147/nss.s401270
8. Sun, H., Ganglberger, W., Panneerselvam, E., Leone, M. J., Quadri, S. A., Goparaju, B., Tesh, R. A., Akeju, O., Thomas, R. J., & Westover, M. B. (2020). Sleep staging from electrocardiography and respiration with deep learning. *Sleep*. https://doi.org/10.1093/sleep/zsz306
9. Redmond, S.J., de Chazal, P., O'Brien, C., Ryan, S., McNicholas, W. T., & Heneghan, C. (2007). Sleep staging using cardiorespiratory signals. *Somnologie 11*. https://doi.org/10.1007/s11818-007-0314-8.
10. Brian, C., Bruce, J. S., & Naresh, M. P. (2010). Utility of sleep stage transitions in assessing sleep continuity. *Sleep, 33*, 1681–1686. https://doi.org/10.1093/sleep/33.12.1681
11. Kawamoto, R., Nazir, A., Kameyama, A., Ichinomiya, T., Yamamoto, K., Tamura, S., Yamamoto, M., Hayamizu, S., & Kinosada, Y. (2013). Hidden Markov model for analyzing time-series health checkup data. *Studies in Health Technology and Informatics, 192*, 491–495. https://doi.org/10.3233/978-1-61499-289-9-491
12. Watkins, R. E., Eagleson, S., Veenendaal, B., et al. (2009). Disease surveillance using a hidden Markov model. *BMC Medical Informatics and Decision Making, 9*, 39. https://doi.org/10.1186/1472-6947-9-39
13. Votsi, I., Limnios, N., Tsaklidis, G., & Papadimitriou, E. (2014). Hidden Semi-Markov modeling for the estimation of earthquake occurrence rates. *Communications in Statistics: Theory and Methods*. https://doi.org/10.1080/03610926.2013.857414.
14. Chen, M.H., Lin, M.J. et al. (2019). Banded Pair-HMM Algorithm for DNA Variant Calling and Its Hardware Accelerator Design. In *2019 IEEE 19th International Conference on Bioinformatics and Bioengineering (BIBE), Athens, Greece*, pp 563–566. https://doi.org/10.1109/BIBE.2019.00107
15. Glennie, R., & Adam, T. (2022). Hidden Markov models: Pitfalls and opportunities in ecology. *Methods in Ecology and Evolution, 14*(1), 43–56. https://doi.org/10.1111/2041-210X.13801
16. Ingmar, V., Maartje, E. J. R., & Peter, C. M. M. (2002). Fitting hidden Markov models to psychological data. *Scientific Programming*. https://doi.org/10.1155/2002/874560
17. Yoon, B. J. (2009). Hidden Markov models and their applications in biological sequence analysis. *Current Genomics, 10*(6), 402–415. https://doi.org/10.2174/138920209789177575
18. Mark, G., & Steve, Y. (2007). The application of hidden Markov models in speech recognition. *Foundations and Trends in Signal Processing,* pp 195–304. https://doi.org/10.1561/2000000004.
19. Huang, H., Zhang, J., Zhu, L., Tang, J., Lin, G., Kong, W., Lei, X., & Zhu, L. (2021). EEG-based sleep staging analysis with functional connectivity. *Sensors*. https://doi.org/10.3390/s21061988
20. Lee, J., Kim, H.C., Lee, Y.J. et al, (2023). Development of generalizable automatic sleep staging using heart rate and movement based on large databases. *Biomedical Engineering Letters*, https://doi.org/10.1007/s13534-023-00288-6.
21. Timplalexis, C. (2018). Classification of Sleep Stages Using Mache Learning Methods, *International Hellenic University,*

School of Science&Technology. https://repository.ihu.edu.gr/xmlui/bitstream/handle/11544/29403/Classification%20of%20Sleep%20Stages%20Using%20Machine%20Learning%20Methods.pdf?sequence=1.
22. Penzel, T., Kantelhardt, J. W., Lo, C. C., Voigt, K., & Vogelmeier, C. (2003). Dynamics of heart rate and sleep stages in normals and patients with sleep apnea. *Neuropsychopharmacology: Official Publication of the American College of Neuropsychopharmacology, 28*(Suppl 1), S48–S53. https://doi.org/10.1038/sj.npp.1300146.
23. Sridhar, N., Shoeb, A., Stephens, P., et al. (2020). Deep learning for automated sleep staging using instantaneous heart rate. *Digital Medicine, 3*, 106. https://doi.org/10.1038/s41746-020-0291-x
24. Katerina, D. T., Athanasios, T., Katerina, T. et al, (2018). EEG-Based Automatic Sleep Stage Classification, *Biomedical*. https://biomedres.us/fulltexts/BJSTR.MS.ID.001535.php.
25. Minecan, D., Natarajan, A., Marzec, M., & Malow, B. (2002). Relationship of epileptic seizures to sleep stage and sleep depth. *Sleep, 25*(8):899–904. https://pubmed.ncbi.nlm.nih.gov/12489898/.
26. Vallat, R., & Walker, M. P. (2021) An open-source, high-performance tool for automated sleep staging. *eLife 10:*e70092. https://doi.org/10.7554/eLife.70092.
27. Pessoa, D., Petmezas G. et al., (2023). Pediatric Respiratory Sound Classification Using a Dual Input Deep Learning Architecture, *2023 IEEE Biomedical Circuits and Systems Conference (BioCAS)*, pp.1–5. https://doi.org/10.1109/BioCAS58349.2023.10388733
28. Baik, K., Jung, J. H., Jeong, S. H., et al. (2022). Implication of EEG theta/alpha and theta/beta ratio in Alzheimer's and Lewy body disease. *Science and Reports, 12*, 18706. https://doi.org/10.1038/s41598-022-21951-5
29. Attar, E. T. (2022). Review of electroencephalography signals approaches for mental stress assessment. *Neurosciences, 27*(4), 209–215. https://doi.org/10.17712/nsj.2022.4.20220025
30. Rani, K. S. S., Raja, S. P., Sinthuja, M., et al. (2022). Classification of EEG signals using neural network for predicting consumer choices. *Computational Intelligence and Neuroscience, 2022*, 5872401. https://doi.org/10.1155/2022/5872401
31. Goldberger, A. L., Amaral, L. A., Glass, L., Hausdorff, J. M., Ivanov, P. C., Mark, R. G., Mietus, J. E., Moody, G. B., Peng, C. K., & Stanley, H. E. (2000). PhysioBank, PhysioToolkit, and PhysioNet: Components of a new research resource for complex physiologic signals. *Circulation, 101*(23), E215–E220. https://doi.org/10.1161/01.cir.101.23.e215
32. Behzad, R., & Behzad, A. (2021). The role of EEG in the diagnosis and management of patients with sleep disorders. *Journal of Behavioral and Brain Science, 11*(10), 257–266. https://doi.org/10.4236/jbbs.2021.1110021
33. Iwagami, M., Seol, J., Hiei, T., Tani, A., Chiba, S., Kanbayashi, T., Kondo, H., Tanaka, T., & Yanagisawa, M. (2023). Association between electroencephalogram-based sleep characteristics and physical health in the general adult population. *Scientific Reports, 13*(1). https://doi.org/10.1038/s41598-023-47979-9
34. Almutairi, H., Hassan, G. M., & Datta, A. (2023). Machine-learning-based-approaches for sleep stage classification utilising a combination of physiological signals: A systematic review. *Applied Sciences, 13*(24), 13280. https://doi.org/10.3390/app132413280
35. Rodríguez-Sotelo, J. L., Osorio-Forero, A., Jiménez-Rodríguez, A., Restrepo-De-Mejía, F., Peluffo-Ordoñez, D. H., & Serrano, J. (2017). Sleep stages clustering using time and spectral features of EEG signals. In Lecture notes in computer science (pp. 444–455). https://doi.org/10.1007/978-3-319-59740-9_44
36. Aboalayon, K., Faezipour, M., Almuhammadi, W., & Moslehpour, S. (2016). Sleep stage classification using EEG Signal analysis: A comprehensive survey and new investigation. *Entropy, 18*(9), 272. https://doi.org/10.3390/e18090272
37. Metzner, C., Schilling, A., Traxdorf, M., Schulze, H., & Krauss, P. (2021). Sleep as a random walk: a super-statistical analysis of EEG data across sleep stages. *Communications Biology, 4*(1). https://doi.org/10.1038/s42003-021-02912-6
38. Horváth, C. G., Szalárdy, O., Ujma, P. P., Simor, P., Gombos, F., Kovács, I., Dresler, M., & Bódizs, R. (2022). Overnight dynamics in scale-free and oscillatory spectral parameters of NREM sleep EEG. *Scientific Reports, 12*(1). https://doi.org/10.1038/s41598-022-23033-y
39. Satapathy, S. K., Brahma, B., Panda, B., Barsocchi, P., & Bhoi, A. K. (2024). Machine learning-empowered sleep staging classification using multi-modality signals. *BMC Medical Informatics and Decision Making, 24*(1). https://doi.org/10.1186/s12911-024-02522-2
40. Papageorgiou, V. (2021). Brain tumor detection based on features extracted and classified using a low-complexity neural network. *Traitement du Signal, 38* 38, 547–554. https://doi.org/10.18280/ts.380302
41. Papageorgiou, V. E., Zegkos, T., Efthimiadis, G., & Tsaklidis, G. (2022). Analysis of digitalized ECG signals based on artificial intelligence and spectral analysis methods specialized in ARVC. *International Journal for Numerical Methods in Biomedical Engineering, 38*(11), e3644. https://doi.org/10.1002/cnm.364
42. Papageorgiou, V.E., Dogoulis, P., Papageorgiou, DP. (2024). A Convolutional Neural Network of Low Complexity for Tumor Anomaly Detection. Proceedings of Eighth International Congress on Information and Communication Technology. ICICT 2023. Lecture Notes in Networks and Systems, 696, Springer, Singapore. https://doi.org/10.1007/978-981-99-3236-8_78
43. Petmezas, G., Haris, K., Stefanopoulos, L., Kilintzis, V., Tzavelis, A., Rogers, J. A., Katsaggelos, A. K., & Maglaveras, N. (2021). Automated atrial fibrillation detection using a hybrid CNN-LSTM network on imbalanced ECG datasets. *Biomedical Signal Processing and Control, 63*, 102194. https://doi.org/10.1016/j.bspc.2020.102194
44. Petmezas, G., Cheimariotis, G., Stefanopoulos, L., Rocha, B., Paiva, R. P., Katsaggelos, A. K., & Maglaveras, N. (2022). Automated lung sound classification using a hybrid CNN-LSTM network and focal loss function. *Sensors, 22*(3), 1232. https://doi.org/10.3390/s22031232
45. Petmezas, G., Papageorgiou, V. E., Vassilikos, V., et al. (2024). Recent advancements and applications of deep learning in heart failure: A systematic review. *Computers in Biology and Medicine, 176*(1), 108557. https://doi.org/10.1016/j.compbiomed.2024.108557